$(H_2O)_{10}$ and $(H_2O)_{12}$ on a Virtual Metal Surface: The Growth of Ice

Henning Henschel and Tobias Krämer

Universität Hamburg, Institut für Physikalische Chemie, Martin-Luther-King Platz 6, D-20146 Hamburg, Germany

Timm Lankau*

c/o Professor Chin-Hui Yu, Department of Chemistry, National Tsing Hua University, 101 KuangFu Road Section 2, HsinChu 30013, Taiwan

Received February 6, 2006. In Final Form: August 26, 2006

$(H_2O)_{10}$ and $(H_2O)_{12}$ are used to investigate the growth of ice on metal surfaces with hexagonal symmetry. The model of the virtual metal surface was used to separate the electronic structure of the metal from that of the water cluster while maintaining the geometric constraints imposed by the metal surface on the water cluster. To complement the ab initio calculations on the water cluster, an additional multicenter analysis was done to analyze the hydrogen bonds within the clusters. These calculations suggested that the water bilayer structure adjacent to the virtual metal surface effectively shields the growing ice cystal from the metal surface.

1. Introduction

A water bilayer structure[1,2] has been proposed as the basis of the growth of ice on hexagonal metal lattices. The ice phase on platinum is believed to have the same hexagonal symmetry as the surface, and a cyclic water hexamer such as that observed in hexagonal ice forms the basis of the bilayer structure.[3] The structure of this water bilayer is generally explained in terms of an extension to surfaces[2] of the Bernal−Fowler−Pauling rules (ice rules).[4,5] Specifically, each water molecule is bound by at least two bonds (which may be hydrogen bonds to other water molecules or oxygen lone pair bonds to the surface) while maintaining a tetrahedral configuration. Each water molecule in the lower layer closest to the metal surface is bound to the surface via a lone pair orbital on the oxygen, and all free lone pair orbitals on oxygen remain nearly perpendicular to the surface. In an ideal infinite bilayer, all water molecules have their dipole moments pointing away from the surface ("flip up"), whereas in a finite cluster, water molecules whose dipole moments point toward the surface ("flip down") may occur at the edge of the cluster.[2,6,7]

A water cluster originating from the described bilayer would have all dipole moments pointing away from the metal surface and thus represents ferroelectric ice. A perfect ferroelectric alignment of the dipole moments is prevented by the aforementioned flip down water molecules at the cluster's edges. Such a species has been observed on Pt(100),[8] and experimental evidence suggests similar water structures on Pt(111).[9,10] Also, two water bilayers can be arranged in a sandwich structure in which the water molecules of the upper bilayer have their dipole moments pointing toward the metal surface.[11] An alternative model for the structure of the water bilayer adjacent to the metal surface has recently been described by Ludwig in his brief review.[12] The dipole moments of the water molecules in the second plane of the bottom bilayer (layer II, Figure 1) point toward the surface as does one OH bond of the water molecule. Such an alignment of the dipole moments preventing the formation of ferroelectric ice clusters can be explained by cooperative contributions to the surface water interaction energy.[13]

In the initial stages of growth, a water molecule has two possible adsorption sites: attached either directly above a platinum atom on the surface or to a water molecule already bound to the surface.[9,14] The coexistence of both species (i.e., a water molecule directly bound to the surface and a water molecule attached to another water molecule) is commonly explained in terms of the energy of isolated bonds, although the importance of cooperative forces has been suggested previously.[10,13,15] The strength of the platinum−water bond corresponds to that of two to three hydrogen bonds, so either type of bonding is possible.

TDS spectra (thermal desorption spectroscopy)[1,9,14,16−23] of water from the platinum(111) surface distinguish different water species. The data from Ogasawara et al.[17] shows three prominent peaks at 155, 165, and 200 K. The first peak (at 155 K) was assigned to ice sublimation, the second (at 165 K), to water in

* Corresponding author. E-mail: lankau@oxygen.chem.nthu.edu.tw (preferred). Phone: (+)886-3-5715131-33414. Fax: (+)886-3-5711082.

(1) Thiel, P. A.; Madey, T. E. *Surf. Sci. Rep.* **1987**, *7*, 211−385.
(2) Doering, D.; Madey, T. *Surf. Sci.* **1982**, *123*, 305−337.
(3) Firment, L. E.; Somorjai, G. A. *Surf. Sci.* **1979**, *84*, 275−294.
(4) Bernal, J. D.; Fowler, R. H. *J. Chem. Phys.* **1933**, *1*, 515−546.
(5) Pauling, L. *J. Am. Chem. Soc.* **1935**, *57*, 2680−2684.
(6) Thiel, P. A.; Hoffmann, F. M.; Weinberg, W. H. *J. Chem. Phys.* **1981**, *75*, 5556−5572.
(7) Lankau, T.; Cooper, I. L. *J. Phys. Chem. A* **2001**, *105*, 4084−4095.
(8) Ibach, H.; Lehwald, S. *Surf. Sci.* **1980**, *91*, 187−197.
(9) Sexton, B. A. *Surf. Sci.* **1980**, *94*, 435−445.
(10) Langenbach, E.; Spitzer, A.; Lüth, H. *Surf. Sci.* **1984**, *147*, 179−190.
(11) Witek, H.; Buch, V. *J. Chem. Phys.* **1999**, *110*, 3168−3175.
(12) Ludwig, R. *Angew. Chem.* **2003**, *42*, 3580−3582.
(13) Lankau, T.; Nagorny, K.; Cooper, I. L. *Langmuir* **1999**, *15*, 7308−7315.
(14) Fisher, G. B.; Gland, J. L. *Surf. Sci.* **1980**, *94*, 446−455.
(15) Miller, J. N.; Ling, D. T.; Stefan, P. M.; Weissman, D. L.; Shek, M. L.; Lindau, I.; Spicer, W. E. *Phys. Rev. B* **1981**, *24*, 1917−1926.
(16) Fisher, G. B. *Monolayer and Multilayer Adsorption of Water on the Pt(111) Surface*; General Motors Research Publication GMR-4007 PCP-171; General Motors Research Laboratories Warren − Physical Chemistry Department: Warren, MI, 1982.
(17) Ogasawara, H.; Yoshinobu, J.; Kawai, M. *Chem. Phys. Lett.* **1994**, *231*, 188−192.
(18) Collins, D. M.; Lee, J. B.; Spicer, W. E. *J. Vac. Sci. Technol.* **1976**, *13*, 266−268.
(19) Fisher, G. B. *Chem. Phys. Lett.* **1981**, *79*, 452−458.
(20) Griffiths, K.; Bonnet, D. *Surf. Sci.* **1986**, *177*, 169−190.
(21) Morgenstern, M.; Michely, T.; Cosma, G. *Phys. Rev. Lett.* **1996**, *77*, 703−706.
(22) Morgenstern, M.; Müller, J.; Michely, T.; Cosma, G. *Z. Phys.* **1997**, *198*, 43−72.
(23) Wagner, F. T.; Moylan, T. E. *Surf. Sci.* **1987**, *191*, 121−146.

10.1021/la0603471 CCC: $33.50
Published on Web 11/14/2006

the second adsorption layer, and the third (at 200 K), to water directly bound to the surface. Whereas the first two peaks have been positively identified, the origin of the third remains a matter of discussion.[21,22,24] The formation of the second peak at 165 K can be observed at coverages as low as 0.13 to 0.27 ideal water bilayer.[2] These TDS results are consistent with other experimental results,[9,10,14,23,25−27] which also support the formation of water clusters at low surface coverage.

The second peak (165 K) is the multilayer peak in the TDS spectrum. A water molecule from the top layer should therefore be in a chemical environment similar to that of an I_h ice crystal. As long as the electronic structure of the surface does not promote a different mechanism of adsorption, such as the dissociative one proposed by Feibelman[28] for Ru(0001), differences in desorption temperature have to be the result of the lattice distortion of the ice crystal because this molecule has no direct contact with the metal below. A measure of this distortion is the lattice-type mismatch (ltm). The highest desorption temperature should therefore be found for the metal with the smallest lattice-type mismatch (copper) but was found for ruthenium. This shift of the maximum peak position and the higher bonding energy compared with that of ice sublimation suggest that the simple bilayer model of Doering and Madey may need further refinement.[7,12,13,29,30]

In contrast, many TDS experiments listed by Thiel and Madey[1] suggest that the formation of the bilayer is very similar on different surfaces whereas ice sublimation examined with ITD (isothermal desorption) experiments[31] has been described as strongly surface-dependent. ITD experiments suggest that ice sublimation depends on the strength of the water−metal interactions up to many water layers on the surface. The surface-independent peak in the ITD spectra has been assigned to amorphous solid water. The surface dependence of ice sublimation is reflected in the number of water layers on the metal surface necessary to observe bulk behavior in the sublimation process in ITD experiments. The number of water layers can be used as a relative measure of the wettability of the surface.[32]

Chakarov[33] and co-workers have examined this effect on the platinum(111) and on the graphite(0001) surface. Bulk behavior of the ice layer was observed at a coverage of at least 30 water monolayers, which contrasts with the value of approximately 5 monolayers by Somorjai.[34] An initial clue to resolve this contradiction is given by another experiment in the same paper. By varying the water deposition temperature between 100 and 135 K, Chakarov et al. were able to show that an amorphous ice peak can no longer be observed in the spectrum and that ice had been formed at the beginning of the experiment, but the typical tailing off of non-zeroth-order desorption kinetics can also be observed in these experiments. Hence, the properties of ice visible in ITD experiments depend significantly on the chosen method of preparation.

Kay et al.[35] showed in their experiments that the sublimation of crystalline ice can be observed in TPD (temperature programmed desorption) spectra even at low deposition temperatures, provided that the surface has been precovered with crystalline ice. The crystalline ice does not induce epitaxial growth of ice if water is deposited at low temperatures but catalyzes the crystallization process. Crystallization rates determined from TPD spectra show that the crystallization of amorphous ice on crystalline ice is about 1000 times faster than that observed on Pt(111).

George et al.[36] reported ITD experiments of H_2O on Ru(001) that show that zeroth-order ice sublimation can be observed even with thin ice films containing more than five water bilayers. Furthermore, their experiments suggest that the vast number of water bilayers necessary to observe bulk behavior[37] can be explained by the surface roughness of the ice film. However, the work of Chakarov, Kay, and co-workers[33,35] suggests that it is possible to observe water desorption from crystalline ice if the ice layers have been carefully prepared. Such preparation should include high adsorption temperatures and long annealing times at temperatures close to that for water desorption. These condition severely limit the number of authentic observations of hexagonal ice on metal surfaces, but two reliable preparations have been reported by Somorjai and co-workers,[27,34] that will be used as an experimental reference in the final discussion (section 5).

2. Surface Model

The geometry of the metal−water interface is controlled by the interaction among three sets of atoms: surface atoms, the water molecules in layer I, and molecules within layers II−IV. To distinguish between these interactions, the model of the virtual surface[7,29,30] was chosen to separate mathematically the growing ice crystal from the electronic structure of the metal surface.

Our model of the metal−water interface used for the calculations reported here comprises three parts: the water bilayer directly attached to the metal surface was represented by a cyclic water hexamer (called bilayer hexagon) with the same geometry as in the bilayer structure proposed by Doering and Madey,[2] the ice crystal was represented by a second water cluster resting on top of the water hexagon, and the metal surface was replaced by a virtual one,[7] which is built from a mesh of seven auxiliary geometrical points and a set of geometry constraints acting on the water cluster. Because the auxiliary geometrical points replace the surface atoms and the hexagonal symmetry of the surface is maintained in all calculations, different metals vary only in the value of the surface lattice constant d_1, defined as the distance between two neighboring auxiliary points (Figure 1).

The water hexamer directly attached to the virtual surface is assumed to have the same geometry as a six-membered water ring in an ideal infinite bilayer structure. Its construction has been described previously,[7,29] and additional information on the geometrical setup is given in Supporting Information. The geometry of a water molecule in the basal plane directly attached to the virtual surface resembles a Lewis-type water−metal bond via an oxygen lone pair. In the second plane, one hydrogen atom of each water molecule lies perpendicular to the virtual metal surface, and the second is used for the hydrogen bond to a water molecule in the basal plane.

(24) Thiam, M. M.; Kondo, T.; Horimoto, N.; Kato, H. S.; Kawai, M. *J. Phys. Chem. B* **2005**, *109*, 16024−16029.
(25) Ogasawara, H.; Yoshinobu, J.; Kawai, M. *J. Chem. Phys.* **1999**, *111*, 7003−7009.
(26) Ranke, W. *Surf. Sci.* **1989**, *209*, 57−76.
(27) Starke, U.; Matere, N.; Barbieri, A.; Döll, R.; Heinz, K.; Van Hove, M. A.; Somoja, G. A. *Surf. Sci.* **1993**, *287/288*, 432−437.
(28) Feibelman, P. J. *Science* **2002**, *295*, 99−102.
(29) Lankau, T. *J. Phys. Chem. A* **2002**, *106*, 6154−6160.
(30) Konrad, O.; Lankau, T. *Chem. Phys. Lett.* **2002**, *359*, 35−40.
(31) Henderson, M. A. *Surf. Sci. Rep.* **2002**, *46*, 1−308.
(32) Löfgren, P.; Ahlström, P.; Chakarov, D. V.; Lausma, J.; Kasemo, B. *Surf. Sci.* **1996**, *367*, L19−L25.
(33) Löfgren, P.; Ahlström, P.; Lausma, J.; Kasemo, B.; Chakarov, D. *Langmuir* **2003**, *19*, 265−274.
(34) Su, X.; Lianos, L.; Shen, Y. R.; Somorjai, G. A. *Phys. Rev. Lett.* **1998**, *80*, 1533−1536.
(35) Dohnálek, Z.; Ciolli, R. L.; Kimmel, G. A.; Stevenson, K. P.; Smith, R. S.; Kay, B. B. *J. Chem. Phys.* **1989**, *110*, 5489−5492.
(36) Livingston, F. E.; Smith, J. A.; George, S. M. *Surf. Sci.* **1996**, *423*, 145−159.
(37) Smith, R. S.; Huang, C.; Wong, E. K. L.; Kay, B. D. *Surf. Sci.* **1996**, *367*, L13−L18.

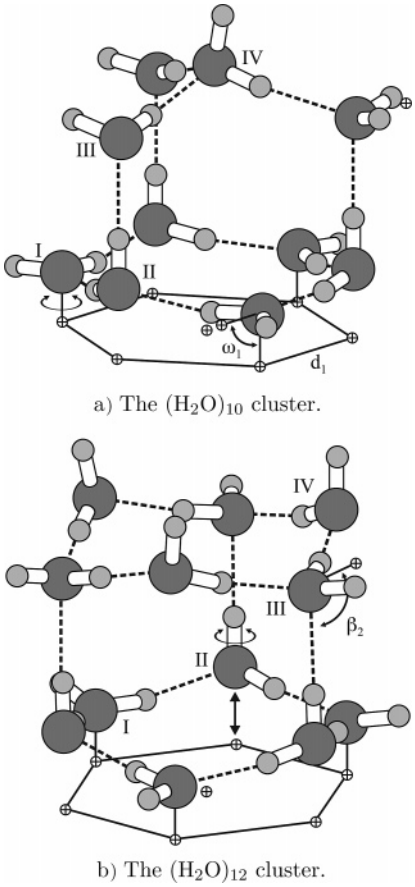

Figure 1. Model cluster for ice growth. Large dark-gray circles mark oxygen atoms, light-gray circles mark hydrogen atoms, and small circles with a cross represent geometrical auxiliary points. The thick dotted lines indicate hydrogen bonds, and the thin solid ones indicate the virtual surface or auxiliary lines. Oxygen atoms marking the planes of the clusters are labeled with Roman numerals.

The water molecules in the first and second planes of the cluster have two degrees of freedom: a water molecule in the first plane has two rotational degrees of freedom, and a molecule in the second plane has one rotational and one translational (Figure 1). The distance between the first and second planes in the optimized water cluster was used as a measure of the nonplanarity of the bilayer hexagon.

The binding energy of a water molecule to an ice crystal is of the order of two to three hydrogen bonds.[1] A water molecule in such an exposed position bound to the water bilayer via three hydrogen bonds can be found at the top of the $(H_2O)_{10}$ cluster (Figure 1a). The water decamer with its adamantane (tricyclo[2.3.1.13,7]decane)-like structure can be found in cubic ice and is therefore a poor model for hexagonal ice on metal surfaces. However, the construction of a water cluster with a similarly exposed water molecule and a structure similar to that observed in hexagonal ice requires many more water molecules, which increases the computational costs beyond a reasonable limit.

The third layer of water molecules in Figure 1a forms the bridge between the molecule at the top and the water bilayer at the bottom. The oxygen atoms of these three water molecules lie at the same height above the corresponding water molecules in the second layer as do their hydrogen atoms. This geometrical constraint forces the bridging water molecules into a geometry similar to that expected for a hydrogen bond to the water bilayer by the lone electron pairs of the bridging water molecules and the hydrogen atoms at the top of the bilayer hexagon. Despite this constraint, the bridging water molecules were allowed to reorient freely during geometry optimizations.

According to the ice rules,[4,5] only two of the three bridging water molecules can point with one of their hydrogen atoms to the top molecule, and both hydrogen atoms of the third bridging water molecule have to point away from the top molecule (Figure 1a). The symmetry of the $(H_2O)_{10}$ cluster is reduced to C_1.

The water dodecamer (Figure 1b) has the correct symmetry to represent hexagonal ice I_h. It was formed from the original model by adding a cyclic hexamer to the bilayer hexagon maintaining C_3 symmetry. This new water hexagon at the top will be called ice hexagon. The three water molecules in the third plane are defined in a fashion similar to those in the cluster of 10: the oxygen atoms of these water molecules stay at the same varying distance from the second layer, but they do not need to stay right on top of an oxygen atom. They were allowed to reorientate under the named constraints during geometry optimizations. The final three water molecules of the dodecamer were allowed to reorient freely under the constraint of C_3 symmetry, which maintains the bilayerlike geometry.

The distance between the oxygen atoms of the water molecules at the top of the ice hexagon and those at the bottom (layer III) is a measure of the nonplanarity of the ice hexagon. Another measure of the nonplanarity of the ring is the angle β_2, which is defined similarly to the angle ω_1 in the bilayer hexagon (Figure 1). β_2 is defined as the angle between the normal of the virtual surface and the symmetry axis of the water molecule.

3. Computational Details

Hartree−Fock (HF) and density functional theory (DFT using the B3LYP hybrid method as defined in Gaussian 98[38]) calculations using Dunning's DZP basis set[39] were performed to compute the total energy of the clusters during geometry optimizations for various values of the surface lattice constant d_1. These calculations were complemented by an analysis of the multicenter energy contributions[29] to the total energy. The multicenter energy calculations were made using a variation of Stillinger's equations,[40] which have been widely used for these purposes.[41−47]

The absolute energy E_{ABS} of a cluster built from N water molecules as a function of the monomer positions ($\mathbf{x}_i$) may be written as the sum of multicenter energies (E_{ic}):

$$E_{ABS}(\mathbf{x}_1...\mathbf{x}_N) = E_{1c} + E_{2c} + E_{3c} + \cdots + E_{Nc} \quad (1)$$

$$= \sum_{1=i}^{N} E^{(1)}(\mathbf{x}_i) + \sum_{1=i<j}^{N} V^{(2)}(\mathbf{x}_i, \mathbf{x}_j) + \sum_{1=i<j<k}^{N} V^{(3)}(\mathbf{x}_i, \mathbf{x}_j, \mathbf{x}_k) + \cdots + V^{(N)}(\mathbf{x}_1...\mathbf{x}_N)$$

In the chosen surface model, the single-molecule energies $E^{(1)}(\mathbf{x}_i)$ are equal to the energies of the free monomers E_1 because the geometry of the water monomers was frozen at its experimentally

(38) Frisch, M. J.; Trucks, G. W.; Schlegel, H. B.; Scuseria, G. E.; Robb, M. A.; Cheeseman, J. R.; Zakrzewski, V. G.; Montgomery, J. A., Jr.; Stratmann, R. E.; Burant, J. C.; Dapprich, S.; Millam, J. M.; Daniels, A. D.; Kudin, K. N.; Strain, M. C.; Farkas, O.; Tomasi, J.; Barone, V.; Cossi, M.; Cammi, R.; Mennucci, B.; Pomelli, C.; Adamo, C.; Clifford, S.; Ochterski, J.; Petersson, G. A.; Ayala, P. Y.; Cui, Q.; Morokuma, K.; Malick, D. K.; Rabuck, A. D.; Raghavachari, K.; Foresman, J. B.; Cioslowski, J.; Ortiz, J. V.; Stefanov, B. B.; Liu, G.; Liashenko, A.; Piskorz, P.; Komaromi, I.; Gomperts, R.; Martin, R. L.; Fox, D. J.; Keith, T.; Al-Laham, M. A.; Peng, C. Y.; Nanayakkara, A.; Gonzalez, C.; Challacombe, M.; Gill, P. M. W.; Johnson, B. G.; Chen, W.; Wong, M. W.; Andres, J. L.; Head-Gordon, M.; Replogle, E. S.; Pople, J. A. *Gaussian 98*; Gaussian, Inc.: Pittsburgh, PA, 1998.

(39) Dunning, T. H., Jr. *J. Chem. Phys.* **1970**, *53*, 2823−2833.

observed values (r_{OH} = 0.9572 Å, $\angle_{HOH}$ = 104.52° [48]). The multicenter energies are given by the sum of the individual multicenter interactions $V^{(i)}(\mathbf{x}_1, ...\mathbf{x}_i)$ and can be calculated recursively according to the following equation.

$$E^{(1)}(\mathbf{x}_i) \equiv E(\mathbf{x}_i) = E_1 \quad (2)$$

$$V^{(2)}(\mathbf{x}_i, \mathbf{x}_j) = E_2(\mathbf{x}_i, \mathbf{x}_j) - E^{(1)}(\mathbf{x}_i) - E^{(1)}(\mathbf{x}_j)$$

$$V^{(3)}(\mathbf{x}_i, \mathbf{x}_j, \mathbf{x}_k) = E_3(\mathbf{x}_i, \mathbf{x}_j, \mathbf{x}_k) - E^{(1)}(\mathbf{x}_i) - E^{(1)}(\mathbf{x}_j) - E^{(1)}(\mathbf{x}_k) - V^{(2)}(\mathbf{x}_i, \mathbf{x}_j) - V^{(2)}(\mathbf{x}_i, \mathbf{x}_k) - V^{(2)}(\mathbf{x}_j, \mathbf{x}_k)$$

$$\vdots$$

To obtain the multicenter interaction energies $V^{(i)}$, the energy ($E_i(\mathbf{x}_1, ...\mathbf{x}_i)$) of a subset of water molecules is needed. During these calculations, the water molecules stay in the same positions ($\mathbf{x}_i$) as in the optimized cluster.

The binding energy of the complete cluster E_{BIND}^{TOT} is the energy difference between E_{ABS} of the cluster and the sum of all monomer energies E_{1c}.

$$E_{BIND}^{TOT}(\mathbf{x}_1,...\mathbf{x}_N) = E_{ABS} - E_{1c} = E_{2c} + E_{3c} + ... + E_{Nc} \quad (3)$$

Whereas E_{BIND}^{TOT} describes the formation of the complete cluster, the binding energy of the first water molecule of the cluster with the remainder can be calculated by summing exclusively over those multicenter interaction energies $V^{(i)}(\mathbf{x}_1, ...\mathbf{x}_i)$ that contain the first molecule $\mathbf{x}_1$:

$$E_{BIND} = E_{2c}^{Int} + E_{3c}^{Int} + \cdots + E_{Nc}^{Int} \quad (4)$$

$$= \sum_{j=2}^{N} V^{(2)}(\mathbf{x}_1, \mathbf{x}_j) + \sum_{2=j<k}^{N} V^{(3)}(\mathbf{x}_1, \mathbf{x}_j, \mathbf{x}_k) + \cdots + V^{(N)}(\mathbf{x}_1...\mathbf{x}_N)$$

All energy calculations were made using the Gaussian 98 program package, and the multicenter energy analysis was done using our own code, which can be obtained from the author upon request.

4. Results

The HF results describe the same chemistry as the DFT calculations. Therefore, only the DFT results are discussed here. For comparison, the HF results are presented in Supporting Information. This section reporting the DFT results is subdivided into two subsections. The first subsection focuses on the geometry of the optimized water clusters, and the energetic effects are discussed in the second one.

4.1. Structural Changes. This section focuses on the geometry of the $(H_2O)_{10}$ and $(H_2O)_{12}$ clusters as a function of the surface lattice constant d_1. Both $(H_2O)_{10}$ and $(H_2O)_{12}$ represent an extension of the bilayer hexagon. A $(H_2O)_6$ cluster has been used previously[7,29] to analyze the properties of the water bilayer on hexagonal metal surfaces. To distinguish this $(H_2O)_6$ cluster from that observed in $(H_2O)_{10}$ and $(H_2O)_{12}$, this water hexamer will be called isolated hexagon within this text.

4.1.1. Geometry of the Bilayer Hexagon. The height h_1 of the isolated bilayer hexagon as a function of the surface lattice constant d_1 has been discussed in detail in ref 7. As the value of d_1 increases, the bilayer hexagon becomes flatter, and at d_1 > 2.7 Å, the bilayer hexagon was approximately planar. Figure 2a compares the results for the height h_1 of the bilayer hexagon obtained for $(H_2O)_6$, $(H_2O)_{10}$, and $(H_2O)_{12}$. Correlation calculations on the isolated $(H_2O)_6$ cluster have been made at the MP2 level,[7] and correlation effects have been included in the calculations for $(H_2O)_{10}$ and $(H_2O)_{12}$ via DFT calculations. The flattening of the bilayer hexagon can be observed in $(H_2O)_{10}$ and $(H_2O)_{12}$, similar to the results obtained for the isolated hexamer as bilayer model. Total planarity ($h = 0$) was not observed within the HF calculations with d_1 < 3.0 Å (Supporting Information).

The agreement among the results for h_1 as a function of d_1 ($h_1(d_1)$) is very good. However, the results for $(H_2O)_{10}$ suggest that the bilayer hexagon in $(H_2O)_{10}$ is slightly more planar than that in $(H_2O)_6$ or $(H_2O)_{12}$. A similar effect can be observed in the tilt (ω_1) of the water molecules in the first layer (Figure 2b).

Regarding the orientation of the water molecules in layer I, all three cluster models show the same behavior. With increasing values of d_1, the tilt ω_1 of the water molecules in the first plane decreases after passing through an initial maximum. For values of d_1 > 2.7 Å, the value of ω_1 becomes smaller than 90°. The increase in cluster size enhances the ice character (ω_1 is closer to its ideal value of 125°) of the bilayer hexagon, but values for ω_1 < 90° can still be observed in $(H_2O)_{10}$ and $(H_2O)_{12}$. The curves for $\omega_1(d_1)$ are nearly the same for $(H_2O)_{10}$ and $(H_2O)_{12}$ for d_1 < 2.5 Å. As d_1 becomes larger than 2.5 Å, the hydrogen atoms of the layer I water molecules in $(H_2O)_{10}$ move faster toward the surface than those in $(H_2O)_{12}$, and the bilayer hexagons of $(H_2O)_6$ and $(H_2O)_{10}$ become more alike. The ice hexagon in $(H_2O)_{12}$ seems to stabilize the ice character of the underlying bilayer hexagon, but it cannot prevent hydrogen atoms of layer I water molecules moving down toward the virtual surface for d_1 > 2.8 Å.

A value smaller than 90° for ω_1 implies that both hydrogen atoms of water molecules in the first layer have to point to the metal surface. This orientation of the hydrogen atoms is unlikely to be observed on a real metal surface because the energy necessary to move both hydrogen atoms into this position increases rapidly as the value of ω_1 falls below 90°.[7,49] Therefore, it seems to be justified to assume that the value of ω_1 does not fall much below 90° and that the movement of the hydrogen atoms in first-layer water molecules stops as approximate planarity is reached.

In summary, parts a and b of Figure 2 demonstrate clearly that the geometry of the bilayer hexagon is affected only to a small extent by the additional water and therefore its geometry seems to be controlled solely by the surface lattice constant d_1.

4.1.2. Geometry of the Ice Hexagon. The height of the ice bilayer, which is defined as distance between planes III and IV, seems to be insensitive of the value of the surface lattice constant d_1 ($\Delta_{max}^{min} \approx 0.06$ Å) as shown in Figure 3a. The height of the ice hexagon ($h_3 \approx 0.69$ Å) is significantly smaller than that expected for an ice structure built from ideal tetrahedra (~1.5 Å), which agrees well with previous calculations[7] that showed that the

(40) Hankins, D.; Moskowitz, J. W.; Stillinger, F. H. *J. Chem. Phys.* **1970**, *53*, 4544−4554.
(41) Xantheas, S. S. *Philos. Mag. B* **1996**, *73*, 107−115.
(42) Xantheas, S. S. *NATO ASI Ser., Ser. C* **2000**, *561*, 119−128.
(43) Hodges, M. P.; Stone, A. J.; Xantheas, S. S. *J. Phys. Chem. A* **1997**, *101*, 9163−9168.
(44) Kim, K. S.; Dupuis, M.; Lie, G. C.; Clementi, E. *Chem. Phys. Lett.* **1986**, *131*, 451−456.
(45) Xantheas, S. S. *J. Chem. Phys.* **1994**, *100*, 7523−7534.
(46) Pedulla, J. M.; Jordan, K. D. *NATO ASI Ser., Ser. C* **2000**, *561*, 35−44.
(47) Pedulla, J. M.; Kim, K.; Jordan, K. D. *Chem. Phys. Lett.* **1998**, *291*, 78−84.
(48) Benedict, W. S.; Gailar, N.; Plyer, E. K. *J. Chem. Phys.* **1956**, *24*, 1139−1165.
(49) Lankau, T. *A* Computational Analysis of the Platinum-Water-Vacuum Interface. Ph.D. Thesis, University of Hamburg, Hamburg, Germany, 2000. http://www.sub.uni-hamburg.de/disse/398/Diss.pdf.

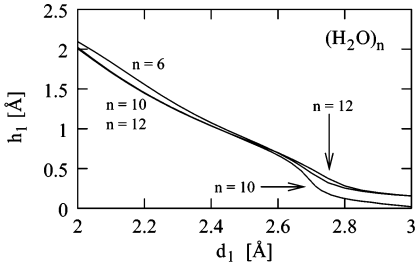

a) Height h_1 of the bilayer hexagon.

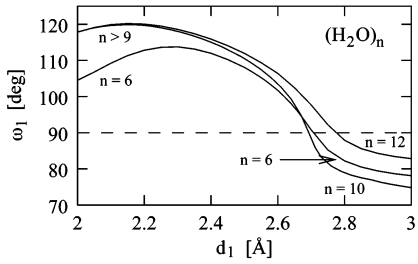

b) Tilt ω_1 of the first layer water molecules.

Figure 2. Geometry changes in the bilayer hexagon as a function of surface lattice constant d_1. Data for $(H_2O)_6$ taken from ref 7.

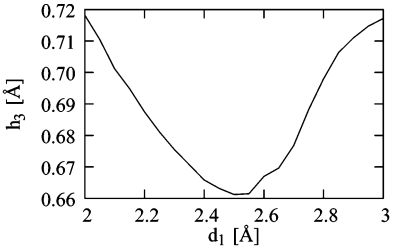

a) Height h_3.

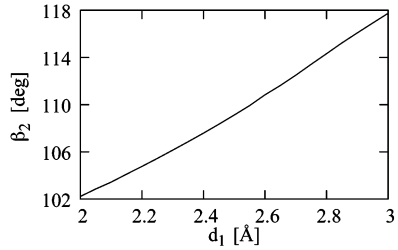

b) Tilt β_2.

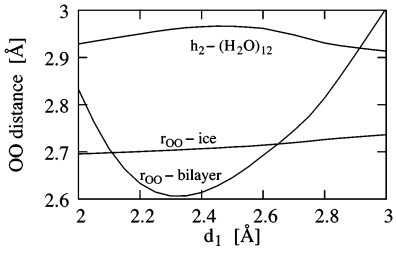

c) Innercluster separation h_2 and hydrogen bond length r_{OO}.

Figure 3. Geometry of the ice hexagon.

hexagon of the isolated hexamer ($h_1 = 0.73$ Å) and that of the free hexamer are also much flatter than expected.

The tilt β_2 (Figure 3b) of the water molecules in the third plane seems to be less dependent on d_1 than that of the molecules in the first plane (ω_1), as a comparison with Figure 2b shows. The value of β_2 increases linearly with the value of d_1, and values of β_2 smaller than 90° were not found. This observation can be

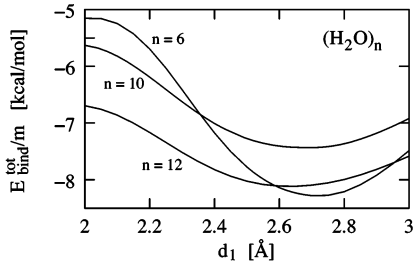

a) Energy of formation per hydrogen bond $E_{\mathrm{BIND}}^{\mathrm{TOT}}/m$; m is the number of hydrogen bonds.

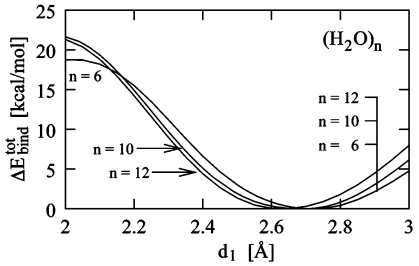

b) Changes in $E_{\mathrm{BIND}}^{\mathrm{TOT}}$ relative to the minimum energy.

Figure 4. Dependency of the energy of formation $E_{\mathrm{BIND}}^{\mathrm{TOT}}$ on d_1. Data for $(H_2O)_6$ taken from ref 7.

explained by the directional hydrogen bonds between the molecules in the second and third planes.

The ice hexagon seems to float above the bilayer hexagon with its geometry frozen close to the optimal one. This floating can be deduced from the graph in Figure 3c, which shows the distance h_2 between planes II and III in $(H_2O)_{12}$. As observed previously for h_3, the value of h_2 varies only slightly with surface lattice constant d_1. The additional water structures always stay at approximately the same distance from the second plane despite the height of the bilayer hexagon.

The oxygen−oxygen distance of hydrogen bonds between direct neighbors (r_{OO}) in the bilayer hexagon depends strongly on d_1. For small values of d_1, r_{OO} is large because the water molecules of the second plane are pushed upward by the compression, and for large values of d_1, r_{OO} is large again because large values of d_1 pull the bilayer hexagon apart, as the water molecules of the first layer have to stay above the virtual surface atoms. This cannot be observed in the ice hexagon. The value of r_{OO} in the ice hexagon is virtually unaffected by the changes in d_1, despite a small increase in r_{OO} for large values of d_1.

A similar effect has been observed in the $(H_2O)_{10}$ cluster. The height (h_3) of the additional $(H_2O)_4$ pyramid as well as its distance from the bilayer hexagon hardly changes with d_1, which suggests that the observed flotation is independent of the structure of the added water cluster.

4.2. Energetic Effects. The analysis of the cluster geometries showed that the ice hexagon and the water tetramer in $(H_2O)_{10}$ seem to float on the bilayer hexagon. This section focuses on the energetic aspects of this floating, the next subsection will focus on the bilayer hexagon, the following two will discuss the bonding energy of water molecules in the fourth layer, and multicenter energy effects are discussed in the final subsection.

4.2.1. Bilayer Hexagon. Figure 4a shows the energy of formation of the complete water clusters $E_{\mathrm{BIND}}^{\mathrm{TOT}}$ divided by the number m of hydrogen bonds in the cluster as a function of surface lattice constant d_1. Because the number of hydrogen

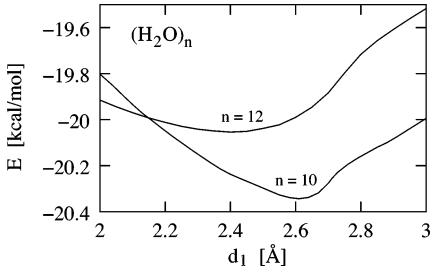

Figure 5. Bonding energy E_{BIND} of a layer IV water molecule.

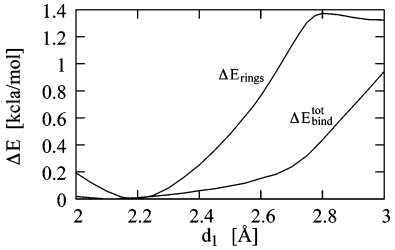

Figure 6. Bonding energy E_{rings} between the bilayer and the ice hexagon and energy of formation E_{BIND}^{TOT} relative to their minima in $(H_2O)_{12}$.

bonds ($(H_2O)_6$:6, $(H_2O)_{10}$:12, $(H_2O)_{12}$:15) does not change during the calculations, Figure 4a can also be used to analyze E_{BIND}^{TOT}.

The resulting curves for E_{BIND}^{TOT}/m for $(H_2O)_{10}$ and $(H_2O)_{12}$ have the same shape as that for $(H_2O)_6$, although their dependence on d_1 is smaller. The additional hydrogen bonds in $(H_2O)_{10}$ and $(H_2O)_{12}$ seem to lessen the influence of d_1 on E_{BIND}^{TOT}. Furthermore, the absolute values of E_{BIND}^{TOT}/m for $d_1 \geq 2.6$ Å indicate that the average hydrogen bond in the small water hexamer is stronger than that in the larger water cluster.

All curves seem to have a maximum close to $d_1 = 2$ Å and a minimum in the range of 2.6 Å $\leq d_1 \leq$ 2.8 Å. The maximum at 2 Å indicates a major change in the bilayer structure, which has been analyzed previously for the isolated $(H_2O)_6$ cluster:[7] the bilayer hexagon turns into a triangular antiprism by splitting into two trimers. The visual inspection of the geometries for $(H_2O)_{10}$ and $(H_2O)_{12}$ reveals a similar transition for small values of d_1. However, the splitting of the bilayer hexgon does not seem to affect the floating ice hexagon.

$\Delta E_{BIND}^{TOT}(d_1)$ is the difference between the value of E_{BIND}^{TOT} at a given value for d_1 and that of E_{BIND}^{TOT} at the energy minimum (Figure 4b). The changes in E_{BIND}^{TOT} for $(H_2O)_{10}$ and $(H_2O)_{12}$ are the same as those observed for $(H_2O)_6$, which suggests that the surface dependency of the energetics in the water cluster are dominated by the bilayer hexagon.

4.2.2. Top Water Molecule. Figure 5 shows the binding energy E_{BIND} of a water molecule from layer IV in the $(H_2O)_{10}$ and the $(H_2O)_{12}$ clusters. The water decamer has been chosen as a surface model to test the effect of the surface lattice constant d_1 on the sublimation energy because the water molecule at the top is bound to the cluster by three hydrogen bonds. The $E_{BIND}(d_1)$ curve of this water molecule has a minimum at 2.61 Å, which agrees fairly well with the minima for the total energy of formation curves E_{BIND}^{TOT} ($d_1 = 2.70$ Å). The cluster lowest in energy binds the top water molecule most strongly as observed previously for a layer II water molecule in the isolated $(H_2O)_6$ cluster.[7]

Experimental data for the formation of ice on a hexagonal metal surface exist for 2.5 Å $\leq d_1 \leq$ 3.0 Å. The changes in E_{BIND} are small in this region of the plot ($\Delta_{min}^{3.0}E_{BIND} = 0.35$ kcal/mol), which suggests that the ice sublimation energy is decoupled from the surface lattice constant d_1.

Figure 5 also includes similar plots for the $(H_2O)_{12}$ cluster. Although a layer IV water molecule is bound to the cluster by only two bonds, the values for E_{BIND} are similar in size. The minima in the $E_{BIND}(d_1)$ curves calculated with the $(H_2O)_{12}$ cluster are much shallower and are found at smaller values for d_1 than those for the $(H_2O)_{10}$ cluster. The value of E_{BIND} decreases continuously in the range of 2.5 Å $\leq d_1 \leq$ 3.0 Å, but these changes, though larger in size, are still comparable to those observed for $(H_2O)_{10}$ ($\Delta_{2.5}^{3.0}E_{BIND} = 0.79$ kcal/mol), which again suggests that ice sublimation from the second bilayer should be independent of d_1.

4.2.3. Ice Hexagon. The energetic changes in the ice hexagon are all very small (Figure 6, energies plotted relative to their minimum value), which has been heralded in Figure 3 by the constancy of its position (h_2) and the geometry (h_3, β_2, r_{OO}) of the ice hexagon.

The energy of formation E_{BIND}^{TOT} of the ice hexagon hardly changes with d_1 and increases constantly in the experimentally accessible region of d_1 values, whereas the interaction energy E_{rings} between both water rings seems to level off at $d_1 = 2.8$ Å. Although these results suggest very weak coupling between d_1 and the energetics in the ice hexamer, this coupling is unimportant with respect to that observed in the bilayer hexagon (Figure 4b).

4.2.4. Multicenter Energies. Figure 4a shows the value of E_{BIND}^{TOT} per hydrogen bond for the complete cluster. For $d_1 > 2.6$ Å, the strongest average hydrogen bond can be observed in the $(H_2O)_6$ cluster, which is the smallest cluster in this study. Cooperative effects are known to be strong in hydrogen-bonded systems.[29,50−54] The strength of an average hydrogen bond should therefore increase with increasing cluster size, but the opposite was observed here. An additional analysis of the multicenter energies (mce) was done to gain further insight into this observation.

Figure 7a shows the mce analysis of E_{BIND}^{TOT} for the complete $(H_2O)_{12}$ cluster. The minimum in $E_{2c}(d_1)$ can be observed at 2.80 Å, and the minimum in E_{BIND}^{TOT} can be observed at 2.65 Å. This shift is caused by strong three-center energies, which have their minimum at 2.40 Å. Multicenter energies of higher order, which still contribute significantly to E_{BIND}^{TOT} (Table 1), have only a negligible influence on the position of the global minimum. The same mechanism can be observed in the bilayer hexagon (Figure 7b). The minimum in $E_{2c}(d_1)$ can be observed between 2.80 and 2.85 Å, that of $E_{3c}(d_1)$, at 2.45 Å, and the minimum of E_{BIND}^{TOT}, at 2.60 Å. These results agree very well with those from the MP2 calculations on the isolated water hexamer on the virtual surface.[29] The minimum in $E_{2c}(d_1)$ has been observed at 2.85 Å, that in $E_{3c}(d_1)$, at 2.45 Å, but that in E_{BIND}^{TOT}, at 2.70 Å. An analysis of the quantum chemical results suggests that the difference in the positions of the minima for $(H_2O)_6$ and $(H_2O)_{10}/(H_2O)_{12}$ have to be attributed to the different computational methods (step size and correlation method) and not to a cluster size effect because the HF results match much better (Supporting Information).

Figure 7c displays the mce as a function of d_1 in the ice hexagon. The individual contributions hardly change with the value of d_1. The strength of E_{2c} increases ($\Delta_{3.0}^{2.0}E_{2c}^{DFT} = -0.86$ kcal/mol) as d_1 increases. This increase in E_{2c} is compensated for by a decrease in E_{3c} ($\Delta_{3.0}^{2.0}E_{3c}^{DFT} = +1.56$ kcal/mol), and thus the absolute value

(50) Gregory, J. K.; Clary, D. C. *J. Phys. Chem.* **1996**, *100*, 18014−18022.
(51) Liu, K.; Brown, M. G.; Saykally, J. R. *J. Phys. Chem. A* **1997**, *101*, 8995−9010.
(52) Yoon, B. J.; Morokuma, K.; Davidson, E. R. *J. Chem. Phys.* **1985**, *83*, 1223−1231.
(53) Belford, D.; Campbell, E. S. *J. Chem. Phys.* **1984**, *80*, 3288−3296.
(54) Berendsen, H. J. C.; Grigera, J. R.; Straatsma, T. P. *J. Phys. Chem.* **1987**, *91*, 6269−6271.

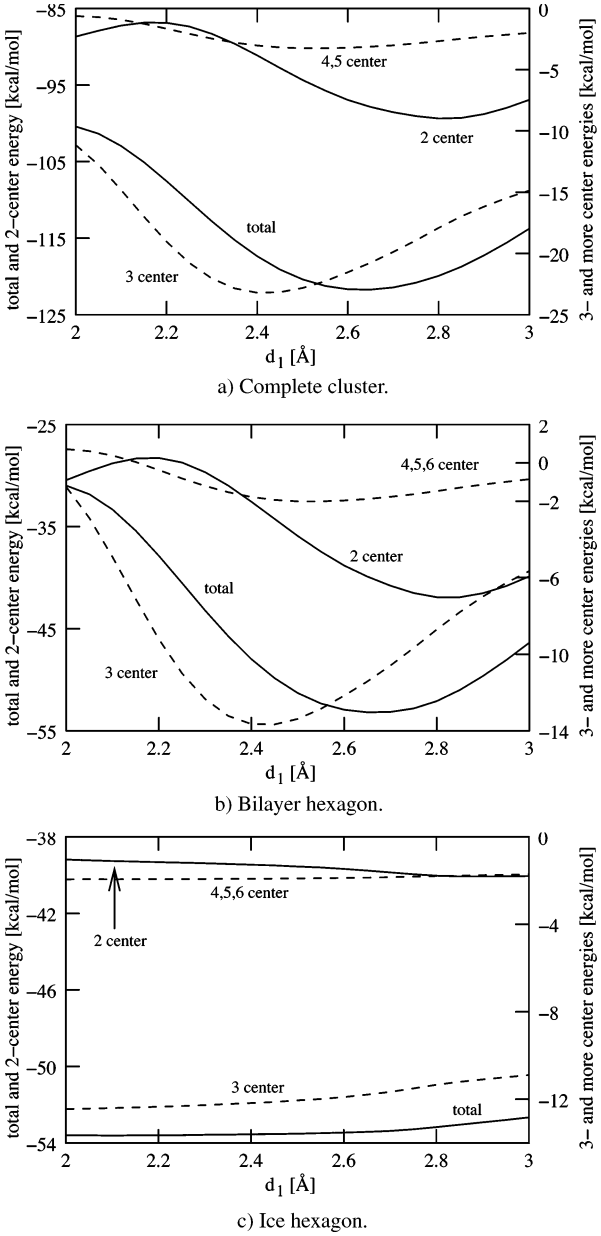

Figure 7. Multicenter energies in $(H_2O)_{12}$. Sums are labeled with a comma: e.g., 4,5 center ≡ sum of 4- and 5-center energy contributions. Total: E_{BIND}^{TOT} of the $(H_2O)_n$ cluster.

Table 1. Multicenter Energies of $(H_2O)_{12}$ at the Global Minimum (d_1 = 2.65 Å)[a]

	complete cluster		bilayer hexagon		ice hexagon	
E_{BIND}^{TOT}	−121.718	100%	−53.195	100%	−53.419	100%
E_{BIND}^{TOT}/m	−8.114		−8.866		−8.903	
E_{2c}	−97.855	80%	−39.888	75%	−39.764	74%
E_{3c}	−20.744	17%	−11.421	22%	−11.791	22%
E_{4c}	−2.873	2%	−1.672	3%	−1.655	3%
E_{5c}	−0.246		−0.203		−0.200	
E_{6c}			−0.011		−0.011	
$\Sigma_{i>3} E_{ic}$	−3.119	3%	−1.886	4%	−1.871	4%

[a] All energies given in kcal/mol.

of E_{BIND}^{TOT} decreases ($\Delta_{3.0}^{2.0} E_{BIND}^{TOT}$ = +0.92 kcal/mol) as d_1 increases. These changes are very small compared to those in the bilayer hexagon, and because the mce pattern reflects chemical bonding within the cluster, it is possible to assume that the bonding mechanism in the ice bilayer is not affected by the changes in d_1.

Table 1 also lists the hydrogen bonding energies in $(H_2O)_{12}$ at the global minimum. The strength of hydrogen bonds in the bilayer and the ice hexagon (−8.9 kcal/mol) is greater than the average bond in the complete $(H_2O)_{12}$ cluster (−8.1 kcal/mol). To lower the average value of the hydrogen bonding energy, the remaining three hydrogen bonds linking the bilayer and the ice hexagon must be weaker than those in the rings. The DFT bonding energy E_{rings} of both rings for d_1 = 2.65 Å is equal to 15.104 kcal/mol. The average strength of a hydrogen bond linking the two hexagons is therefore −5.03 kcal/mol. Calculating the sums along the rows of Table 1 shows that the two-center contributions to the hydrogen bonds are of similar size (bilayer hex., −6.6 kcal/mol; ice hex., −6.6 kcal/mol; link, −6.1 kcal/mol) but the three-center contributions differ in sign (bilayer hex., −1.9 kcal/mol; ice hex., −2.0 kcal/mol; link, +0.8 kcal/mol). The positive sign of E_{3c} suggest that cooperative interactions between the two water rings are disfavored in the chosen geometry of the $(H_2O)_{12}$ cluster, which finally results in a weakening of the hydrogen bond network in the complete cluster itself.

5. Discussion

Table 2 summarizes the results for all water clusters discussed here. Data for an ideal ice I_h structure are given for comparison in the first part of the Table. Ideal ice I_h is made from tetrahedral water molecules, and the lengths of the crystallographic unit cell are used to compute bond distances in this ice model.

According to the model of epitaxial growth, hexagonal ice should grow best on a surface with a lattice constant d_1 of 2.6 Å. The second part of Table 2 contains data for this value of d_1. The height h_1 of the bilayer hexagon is too small. Similar behavior can be observed in the hydrogen bond length in the bilayer hexagon r_{OO}^{bil}, which is also too short (2.69 Å). Better agreement between the ideal and calculated values for the hydrogen bond lengths can be observed in the ice hexagon (2.71 Å), which is still too flat (h_3 = 0.67 Å). Furthermore, the hydrogen bonds perpendicular to the virtual surface are too long (2.96 Å).

The tilts ω_1 and β_2 of the water molecules in layers I and III can be used as a measure of the ice character of the clusters. The value of ω_1 is too small for an icelike structure regardless of cluster size, but a small increase in ω_1 with cluster size (101.7° < 102.6° < 106.4°) can be observed.

Data obtained at the global minimum of E_{BIND}^{TOT} are listed in the third part of Table 2. The value of d_1 at the global minimum decreases slowly toward the ideal value of 2.60 Å as the cluster size increases. This trend can also be seen in the curvature of the $\Delta E_{BIND}^{TOT}(d_1)$ plots (Figure 4b). The value of d_1 at the global energy minimum is always larger than 2.60 Å, and the values for h_3 and ω_1 are therefore smaller than those observed for d_1 = 2.60 Å (Figures 2a and 2b). The decline in these values suggest a less ice-like structure compared with those at d_1 = 2.60 Å. However, the value of ω_1 increases with increasing cluster size, and the hydrogen atoms of the layer I water molecules in $(H_2O)_{12}$ no longer point toward the surface.

A comparison of the geometrical properties of $(H_2O)_n$ (n = 6, 10, 12) with those for ice I_h indicates that the ice character of the clusters increases with cluster size. However, the influence of the cluster size on the cluster geometry is much smaller than that of the surface lattice constant d_1.

Witek and Buch[11] reported molecular dynamics simulations of the ice film on Ru(001) (d_1 = 2.71 Å). The computational setup for an ice film comprising two bilayers was similar to the ideal structure of ferroelectric ice I_h as carried out here for $(H_2O)_{12}$. The authors observed in their simulations the formation of a new structure, which they called a sandwich structure. The dangling

Table 2. Properties of the Complete $(H_2O)_n$ (n = 6, 10, 12) Cluster[a]

		d_1	h_1	h_2	h_3	r_{OO}^{bil}	r_{OO}^{ice}	ω_1	β_2	E_{BIND}^{TOT}	E_{BIND}^{TOT}/n	E_{BIND}^{TOT}/m	E_{2c}	E_{3c}	E_{bind}	E_{rings}
ideal	exp	2.60	0.92	2.75	0.92	2.75	2.75	125	125						−11	
$(H_2O)_6$	MP2	2.60	0.70			2.68		101.7		−48.822	−8.137	−8.137	−36.15	−11.15		
$(H_2O)_{10}$	DFT	2.61	0.64	2.93	0.97	2.69		102.6		−88.945	−8.894	−7.412	−75.19	−12.14	−20.34	
$(H_2O)_{12}$	DFT	2.60	0.70	2.96	0.67	2.69	2.71	106.4	110.8	−121.658	−10.138	−8.111	−96.95	−21.53	−19.99	−15.27
$(H_2O)_6$	MP2	2.70	0.44			2.74		90.8		−49.667	−8.278	−8.278	−38.42	−9.86	−18.20	
$(H_2O)_{10}$	DFT	2.70	0.33	2.91	0.87	2.70		88.5		−89.188	−8.919	−7.433	−76.64	−11.01	−20.28	
$(H_2O)_{12}$	DFT	2.65	0.60	2.95	0.67	2.72	2.72	102.4	111.6	−121.718	−10.142	−8.114	−97.85	−20.74	−19.95	−15.09

[a] All distances (d_1, h_1, h_2, h_3, r_{OO}^{bil}, r_{OO}^{ice}) in are Å, all angles (ω_1, β_2) are in degrees, and all energies (E_{BIND}^{TOT}, E_{BIND}^{TOT}/n, E_{BIND}^{TOT}/m, E_{2c}, E_{3c}, E_{BIND}, E_{rings}) are in kcal/mol. n, number of water molecules; m, number of hydrogen bonds; r_{OO}^{bil}, oxygen−oxygen distance in the bilayer hexagon; r_{OO}^{ice}, oxygen−oxygen distance in the ice hexagon. n, number of molecules and m, number of hydrogen bonds, ideal: parameters calculated assuming an ideal tetrahedral configuration for water and checked with ref 63, and the experimental value for E_{bind} is the averaged value from the 44 to 48 kJ/mol published by Thiel and Madey.[1] Data for $(H_2O)_6$ taken from ref 7.

hydrogen atoms of layer IV water molecules penetrated the ice hexagon; consequently, the number of hydrogen bonds between both bilayers doubled. This movement was not observed during the geometry optimization of $(H_2O)_{12}$ or during the simulations of the ice I_h(0001) surface by Van Hove et al.,[55] who reported a full bilayer termination of the crystal. The simulations of surface melting on ice crystals published by Kroes[56] do not provide evidence for the formation of a sandwich structure, whereas structures akin to the sandwich structure have been observed in simulations by Tanaka, Koga, Zangi, and Mark.[57−59] The energy difference between the ferroelectric conformation and the sandwich structure is about 0.1 kcal/mol per water molecule,[11] and it may be possible that the observation of a ferroelectric → sandwich transition or its absence is caused by either the chosen water−water interaction potential or the computational setup of the water layers. The C_3 symmetry constraint in the construction of $(H_2O)_{12}$ prevents lateral motions of the ice hexagon as observed in neutron scattering experiments[60] and simulations[61] and prevents the complete loss of any structure in the first two bilayers as reported by Nutt and Stone[62] in their study of ice nucleation.

Three types of hydrogen bonds are listed in Table 2: r_{OO}^{bil} is the oxygen−oxygen distance of a hydrogen bond in the bilayer hexagon, r_{OO}^{ice} is the oxygen−oxygen distance in the ice hexagon, and h_2 is distance between the planes of oxygen atoms in layers II and III. r_{OO}^{bil} and r_{OO}^{ice} are equal at the global minimum whereas the value of h_2 is always larger than those two. Small differences in the length of hydrogen bonds along the c axis of the I_h ice crystal and within the hexagons at the crystals basal plane have been reported by Nield et al.[60] This difference (at most 0.03 Å) is much smaller than the differences observed here, which may be attributed to the limited size of the cluster model.

The good agreement of the oxygen−oxygen distance in the quantum calculations at the global minimum (2.74, 2.70, and 2.72 Å) with the experimental value (2.73 to 2.77 Å[60]) and the ideal one of 2.75 Å seems to be fortunate because hydrogen bond lengths are very sensitive to the chosen computational method. Li et al.[63] reported a value of 2.56 Å in their quantum chemical study of I_h ice, whereas molecular mechanics simulations report average oxygen−oxygen separations of 2.7 Å,[64] 2.79 Å (antiferroelectric), and 2.84 Å (ferroelectric).[52]

The binding energy E_{BIND}^{TOT} of the water clusters increases with size, and a similar effect can be observed in the total bonding energy per water molecule E_{BIND}^{TOT}/n, where n equals the number of water molecules in the cluster (Table 2). The optimized values of E_{BIND}^{TOT}/n for $(H_2O)_6$ (MP2, −8.3 kcal/mol) and $(H_2O)_{10}$ (DFT, −8.9 kcal/mol) are very much alike compared to the one for $(H_2O)_{12}$ (DFT, −10.1 kcal/mol). Kim et al.[65,66] reported a saturation of E_{BIND}^{TOT}/n for n = 6 in 2D and for n = 10 in 3D structures. The E_{BIND}^{TOT}/n values suggest that the additional water molecules stabilize $(H_2O)_{12}$ much stronger than they do $(H_2O)_{10}$. Table 2 also displays the strength of an average hydrogen bond within the cluster E_{BIND}^{TOT}/m where m equals the number of hydrogen bonds, which indicates that the average hydrogen bond in $(H_2O)_{12}$ is not exceptional strong but that in $(H_2O)_{10}$ is exceptional weak. The multicenter energy analysis of $(H_2O)_{12}$ showed that the hydrogen bonds linking both water hexagons are weaker than the bonds within the hexagons. Such an anisotropy in bonding energies can also be observed in the mechanical properties of ice[67,68] because the critical resolved shear stress for a nonbasal slip is at least 60 times larger than that for a basal slip in an ice single crystal.

Water desorption from icelike layers of water on hexagonal surfaces can be observed in TPD spectra as a peak with its maximum between 150 and 160 K.[1] The corresponding values of the heats of sublimation lie between 10.5 and 11.5 kcal/mol regardless of the chosen metal surface, which correspond to the strength of two hydrogen bonds and are therefore significantly smaller than the bonding energy of the water molecule at the top of the $(H_2O)_{10}$ cluster.

The surface-independent peak in ITD experiments seems to originate from amorphous solid water whereas the number of water layers on the surface necessary to observe bulk behavior has been described as strongly surface-dependent.[31]

Both experiments, TPD and ITD, conclude with contradicting descriptions of ice formation on a hexagonal metal surface. The discrepancy between both observations may be explained by differences in ice preparation, as suggested in the Introduction.

The preparation of ice on a hexagonal platinum surface reported by Somorjai et al.[27] included an annealing procedure at 140 K.

(55) Materer, N.; Starke, U.; Barbieri, A.; Van Hove, M. A.; Somorjai, G. A.; Kroes, G.-J.; Minot, C. *J. Phys. Chem.* **1995**, *99*, 6267−6269.
(56) Kroes, G.-J. *Surf. Sci.* **1992**, *275*, 365−382.
(57) Koga, K.; Zeng, X. C.; Tanaka, H. *Phys. Rev. Lett.* **1997**, *79*, 5262−5265.
(58) Tanaka, H.; Yamamoto, R.; Koga, K.; Zeng, X. C. *Chem. Phys. Lett.* **1999**, *304*, 378−384.
(59) Zangi, R.; Mark, A. E. *J. Chem. Phys.* **2003**, *119*, 1694−1700.
(60) Nield, V. M.; Whitworth, R. W. *J. Phys.: Condens. Matter* **1995**, *7*, 8259−8271.
(61) Brodholt, J.; Sampoli, M.; Vallauri, R. *Mol. Phys.* **1995**, *85*, 81−90.
(62) Nutt, D. R.; Stone, A. J. *Langmuir* **2004**, *20*, 8715−8720.
(63) Morrisaon, I.; Li, J.-C.; Jenkins, S.; Xantheas, S. S.; Payne, M. C. *J. Phys. Chem. B* **1997**, *101*, 6146−6150.
(64) Sciotino, F.; Corongiu, G. *J. Chem. Phys.* **1993**, *98*, 5694−5700.
(65) Lee, H. M.; Suh, S. B.; Lee, J. Y.; Tarakeshwar, P.; Kim, K. S. *J. Chem. Phys.* **2000**, *112*, 9759−9772.
(66) Lee, H. M.; Suh, S. B.; Lee, J. Y.; Tarakeshwar, P.; Kim, K. S. *J. Chem. Phys.* **2001**, *114*, 3343.
(67) Schulson, E. M. *JOM* **1999**, *51*, 21−27. http://www.tms.org/pub/journals/JOM/9902/Schulson-9902.html.
(68) Duval, P.; Ashby, M. F.; Anderman, I. *J. Chem. Phys.* **1983**, *87*, 4066−4074.

A water dosage of 20 langmuirs created an ice layer thick enough to block electron diffraction from the substrate, and the authors observed a sharp LEED pattern of a $(\sqrt{3} \times \sqrt{3})R30°$ structure. The unit vector of this structure is 4.8 Å, which relates to a value of 2.77 Å for d_1. This d_1 value is significantly larger than that observed in I_h ice (2.61 Å) or that observed in the optimized $(H_2O)_{12}$ cluster (2.65 Å) but corresponds to a platinum−platinum separation of 2.775 Å.[69] These data suggest that the lattice spacing on the platinum surface is maintained in the ice crystal and supports the idea of a strong surface dependence on ice crystallization.

The values of the hydrogen bond lengths in the bilayer and in the ice hexagon (r_{OO}^{bil}, r_{OO}^{ice}) are similar for $d_1 = 2.65$ Å (Figure 3c), and the lateral strain in the ice hexagon should therefore be small for $d_1 \approx 2.6$ Å. For $d_1 = 2.75$ Å, r_{OO}^{bil} equals 2.78 Å, and r_{OO}^{ice} equals 2.72 Å. It is possible to calculate from the hydrogen bond length (r_{OO}) and the height of the cluster (h_3) the value of d_1 for that virtual surface that represents the best geometrical fit to the water hexagon under observation. This calculation yields a value of 2.63 Å for the hypothetical surface under the ice hexagon, which should be compared with 2.75 Å for the bilayer hexagon and 2.6 Å observed in an ideal ice crystal.

The analysis of the $(H_2O)_{12}$ cluster showed that the geometry of the ice hexagon is hardly affected by the virtual surface. A mismatch of 4.3% in the values for d_1 of the bilayer and the ice hexagon could be the source of strong lateral strains in the ice hexagon. These strains are not compensated for in our surface model by interactions normal to the virtual surface as indicated by the floating structure but can be released by domain and/or cluster formation.

Cluster formation on Pt(111) from low water coverage of up to four bilayers has been analyzed by Ogasawara et al.[17] An inspection of their TPD spectra suggests that the maximum of the ice peak (155 K) would not change with the deposition of more water layers, which would suggest bulk behavior although the water has been deposited at 84 K. For water coverages smaller than four bilayers, Ogasawara et al.[17] report the formation of water clusters and small icebergs on the surface. The dependence of the formation of the initial bilayer on the surface lattice constant has been discussed elsewhere,[30] and the movement of water molecules on the basal plane of I_h ice has been examined by Batista and Jónsson.[70]

Batista and Jónsson showed that a single water molecule tries to build up to three hydrogen bonds with surface water molecules, which allows the ad-molecule to occupy noncrystallographic sites. The reported binding energies at the most favorable of these sites vary between 13.4 and 15.2 kcal/mol, whereas the calculations on $(H_2O)_{10}$ predict the bond to be significantly stronger (19.8 to 20.3 kcal/mol, Figure 5). The value of E_{BIND} does not change much ($\Delta E_{BIND} = 0.35$ kcal/mol) for 2.5 Å $\leq d_1 \leq$ 3.0 Å. The ability of hexagonal hydrogen bond networks to detach the bond of a single molecule from innercluster strains in short intermolecular distances can be used to explain the similarity in water binding energies in ice films with more than one bilayer. This property of the hydrogen bond network is also reflected in the similarity of the ice peaks in TPD experiments.

The observed detachment of the additional water structures from the bilayer hexagon can cause lateral strains. As the number of water layers on the metal surface increases, additional vertical hydrogen bonds will be formed that can stabilize the ice layer. It is therefore possible that three or more bilayers of water molecules are necessary to observe bulk properties in the ice film. Below this critical number of layers, the lateral strains can disrupt the ice film, and water clusters or smaller ice domains will be formed from the ice film. Very slow growth conditions as used by Somorjai et al.[27] in their preparation may prevent this disruption and thereby the formation of amorphous solid water because the water molecules can move to their crystallographic sites. Further evidence for the necessity of careful preparation is given by the simulations of Batista and Jónsson, who showed that the new water molecules will add first to noncrystallographic sites and these structures transform later into ice.

The critical number of ice films to shield effectively surface effects is likely to be close to five as suggested by the experiments of Somorjai[34] and George.[36] Somorjai et al.[34] reported another careful preparation of an ice layer on Pt(111) at high temperatures with an additional annealing treatment. The reported TPD spectra suggest that bulk behavior in the ice peak (162 K) can be observed from a surface coverage of approximately five bilayers. The same number of layers has been reported by George et al. from ITD experiments of very smooth water films on Ru(001).

The assumption of five monolayers is further supported by molecular dynamics simulations[56,71] of the ice−water interface. The bilayer peaks in the oxygen density profiles along the ice *c* axis show typical fine structure that reflects the height of a bilayer (h_1 and h_3 in our model). If this fine structure is chosen as a measure of the bilayer's ice character, then these results also suggest that bulk character is restored with the fifth bilayer as observed on metal surfaces.

All of these results suggest that the critical number of water layers is dominated by the hydrogen bond network and only to a small extent by the surface underneath as observed here in the floating of the ice hexagon.

6. Conclusions

The calculations on $(H_2O)_{10}$ and $(H_2O)_{12}$ on the virtual metal surface with respect to the geometry and chemical bonding in water clusters growing on an ideal bilayer structure show detachment from geometrical strains in the bilayer water hexagon directly attached to the metal surface. The additional water structures seem to float on the initial bilayer hexagon, which agrees with the observed surface independence of the ice sublimation peak in TDS spectra. As a result of this detachment, the bilayer hexagon and the ice hexagon have different diameters, which can be a source of lateral strain in the ice layers. These strains are absent in the water bilayer, which can be represented by an isolated $(H_2O)_6$ cluster because the diameter of the bilayer hexagon follows that of the surface hexagon. The emergence of lateral strains in the second bilayer may be the reason for the formation of amorphous solid water on hexagonal metal surfaces.

Acknowledgment. This work is part of T.L.'s habilitation thesis, which has been sponsored by the Job-Foundation. Furthermore, we thank K. Nagorny in Hamburg (D) and I. L. Cooper in Newcastle upon Tyne (GB) for their help within the project.

Supporting Information Available: Details of the model. This material is available free of charge via the Internet at http://pubs.acs.org.

LA0603471

(69) Winter, M. WebElements Periodic Table. http://www.webelements.com.
(70) Batista, E. R.; Jónsson, H. *Comput. Mater. Sci.* **2001**, *20*, 325−336.
(71) Karim, O. A.; Haymet, A. D. J. *J. Chem. Phys.* **1988**, *89*, 6889−6896.